Advances in Science and Technology Research Journal

Advances in Science and Technology Research Journal, 2026, 20(3), 365–372
https://doi.org/10.12913/22998624/214297
ISSN 2299-8624, License CC-BY 4.0

Received: 2025.09.24
Accepted: 2025.12.16
Published: 2026.02.01

Experimental and statistical assessment of starch-modified foam glass for sustainable insulation

Mustafa A. Mohammed[1*], Noor Hatem[2], Safaa Kh Al-Jumaili[1], Mohammed Y. Yousif[1], Eman A. Dh.[1], A. Q. Rawaa[1]

[1] Department of Materials, Engineering College of Engineering, University of Basrah, Basrah, Iraq
[2] Department of Petroleum, Engineering College of Engineering, University of Basrah, Basrah, Iraq
* Corresponding author's e-mail: mohammed.abedlhafd@uobasrah.edu.iq

ABSTRACT

The increasing production of fly ash and waste glass causes serious environmental challenge because of their permanency and potential toxicity. The recycling of these wastes to valuable products is a sustainable way for waste utilization. In the present work, starch was used as a natural porosity enhancer additive in producing fly ash–waste glass foam glass (FAGF) for thermal insulation. Sintering opened the pores to retain their original skeletal network; as a result, sponge-like foams were obtained. The waste glass was ground and filtered on the sieve with a 105 µm hole. A composition of waste glass, flying ash, silicon carbide (SiC) and rice starch was mixed in the required weight ratios. First, the mixture was pelletized using a mold to have a specific shape, and then sintering was carried out at 900 °C. Six formulations with different starch contents (0–6 wt%) had been formulated and tested for density, water absorption, compressive strength and thermal conductivities. The simple weight gain test fully demonstrates that high starch content contributes to higher porosity and lower density, thermal conductivity at the cost of moderate mechanical strength and increased water absorption. The optimum mixture with 6% starch had the minimum thermal conductivity of 0.10875 W/m·K, and acceptable compressive strength (8.66 MPa). This research showed that starch-modified FAGF could be an environmentally-friendly and adjustable insulation material using industrial and agricultural waste as raw materials.

Keywords: fly ash, foam glass (FAGF), starch, compressive strength, thermal conductivity, statistical analysis.

INTRODUCTION

Society and the environment increasingly face issues with waste material. The overproduction of waste, including plastics, electronic debris, and toxic substances, contributes to pollution, resource depletion, and health risks. Plastics persist in the environment for decades, threatening wildlife, and aquatic species (1). The collection and treatment of household and industrial waste, considering human beings and environment is still a great societal challenge. Fly ash, a controlled grain size of particulate by-product from coal burning in power plants; and waste glass obtained from used glass products represent serious environmental hazards because of their accumulation as well as potential leaching into the environment.

Coal fly ash from thermal power plant production causes environmental problems and it is classified as hazardous waste due to high chloride and heavy metals content. Its round particles are mainly composed of aluminum oxide (Al_2O_3), silicon dioxide (SiO_2), calcium oxide (CaO) and iron oxide Fe_2O_3. The chemical composition of fly ash depends on coal origin and combustion process (2). South Korea, which has been burning solid wastes including a large amount of hazardous substances (e.g.dioxins and heavy metals) over 7.3 million tons of coal fly ash was generated via combustion (3). In 2019, China generated a total of 242.06 million tons of MSW, increasing by 153.16% over the level in 2010. The municipal solid waste incineration (MSWI) process generates 1–3% of raw MSWs as fly ash (4). In India,

it was 217.04 in 2018–19 (5). On the other hand, waste glass is a major constituent of solid waste streams and cause both environmental problems and resource management opportunities. According to a report by the United States Environmental Protection Agency (EPA) which measures municipal solid waste (MSW), glass percent was ~12.2 million tons (4.2%) (6).

These waste materials can be utilized in many fields, thus saving resources and protecting the environment as well as promoting sustainable environmental practices. For instance, fly ash can be a supplementary cementitious material in the manufacturing of cement (7), cemented backfill materials (8), bricks (9), and tiles (10). It can also be used to restore degraded areas (11). Similarly, waste glass can be recycled and employed as an alternative for natural concrete aggregates in construction projects (12), concrete pavements (13), asphalt (14), as well as in tile (15) and brick manufacturing (16). One of the most impactful uses of solid waste is the production of foam glass, achieved by combining waste glass powder with fly ash (17). Foam ceramics derived from this provide many advantages, including low density, excellent thermal stability, and a high specific surface area, so that they are suited to applications like insulation and high-temperature catalyst support (18).

The fly ash glass foam (FAGF) begins with fly ash, waste glass, and forming agent. The foaming agent has a crucial function in the FAGF microstructure and properties (19). When preparing FAGF, glass particles and foaming ingredients are sintered to generate a gaseous phase during foam production and form a continuous sintered body when the temperature of the mixture achieves the softening temperature. Softening glass insulates pore-forming agents; gas emission causes glass melt foaming and pores in the sintered body where the pore-forming agent particles were occluded by heating. Foaming agents decompose or oxidize (20). Research suggests that increased porosity lowers thermal conductivity, supporting the use of nanoporous (21, 22) and mesoporous (23) structures. One study found that porosity reduces thermal conductivity and enhances electrical resistivity by impeding the movement of carriers and phonons (24). Additionally, higher porosity in materials creates more insulating contact points. In nanocrystalline materials, porosity can decrease the mean free path of specific phonon modes, further reducing thermal conductivity (25, 26). Foam materials are therefore suitable for thermal insulation due to their closed-pore structure (19).

Within this context, starch is a natural, low-cost pore-forming additive that can be exploited to tune the pore architecture during sintering. Prior studies on foam glass from waste glass and fly ash report the general trade-off between enhanced porosity (improved insulation) and reduced mechanical performance (17–20, 24–26), yet systematic quantification of starch addition in fly ash–waste glass systems – overing density, water absorption, compressive strength, and thermal conductivity and validated by statistical analysis – remains limited. Clarifying this relationship is important for guiding the design of environmentally friendly, effective insulating materials derived from industrial and agricultural wastes.

Accordingly, the study manufactures a range of fly ash–waste glass foam glass incorporating controlled starch (0 to 6 wt%) by a simple mixing–pressing–sintering route; measures density, water absorption, compressive strength and thermal conductivity; and statistically evaluates trends (regression/ANOVA). The working hypothesis is that the increase in porosity by increasing starch content leads to lower thermal conductivity combined with compressive strength (for insulation-cum-strength foams) and results in tunable management of foam glass for an engineering outlet towards sustainability.

MATERIALS AND METHODS

Materials

Silicon carbide SiC (d 50 ≈ 3.5 μm, ≥ 99.5 wt%(, sigma Aldrich and rice starch ≥ 99%, were used as received and stored closed off. Post-consumer soda-lime waste glass (105 mesh) and fly ash, Basrah power plant were washed with water and dried in the oven until dry. Main equipment: planetary ball mill (Japan), 105 mesh sieve (SPY, Japan), uniaxial press (China), box resistance furnace (China) and universal testing machine (UTM) (Suns., Shenzhen, China, Series SKZ1061C, mfg. 2024).

Methodology

The waste glass, which mainly are chipped off bottles first is crushed and reduced into pieces. These particles are ground to comminute

the glass into powder, and sieved by a mesh to have different size of particles. In this study, 105-mesh glass powder was used. The proportions of components for each sample are shown in Table 1. The initial three sets of samples (S1, S2, and S3) were developed by mixing various combinations of glass and fly ash, whereas the latter three groups of samples (S4, S5, and S6) were made by blending the optimized ratios of blended powder with varied dosages of starch.

The next step involved mixing waste glass, fly ash, and SiC in a ball mill for two hours. Porcelain jars using a planetary ball mill were used to homogenize the raw material mixtures. After blending, ten drops of oil were added while mixing. The prepared batches were shaped into disks measuring 22 mm in diameter and 10 mm in thickness through uniaxial dry pressing at a pressure of 10 MPa. The powder was then compacted using a cold press at 5 tons of pressure for 3 minutes. The samples were dried at 120 °C for four hours in an oven before sintering in a furnace set to 900 °C for 45 minutes. Once the sintering was complete, the samples were allowed to cool naturally inside the stove.

Starch is a pore-forming agent. To prepare pellets (S4, S5, and S6), the bulk material was preheated to 650 °C for 6 hours before sintering to ensure the starch was burned out. The powder density and bulk density of the materials were measured using the a 50 ml pycnometer and the Archimedes method, respectively. The foam sample compressive strength was evaluated with a universal testing machine (Suns, Shenzhen, China) operating at a 2 mm/min crosshead speed.

All raw materials were kept and stored in polyethylene bags under-seal at room temperature from moisture. Post consumer waste glass (bottle glass) was rinsed, oven dried, crushed and sieved to 105 mesh; fly ash used as received and stored in sealed condition. All powders were oven-dried (≈120 °C, 4 h) until constant weight before weighing them. Batch compositions are given in Table 1 (SiC kept constant at 0.3 g; starch, 0, 2, 4 and 6 wt.% with respect to the total solids). Powders were weighed by an analytical balance (±0.1 mg), and mixed in porcelain pot with a planetary ball mill with porcelain jars, 2 h and very little (~10 drops) of oil was added to the mixtures as lubricant in mixing. The green bodies (Ø 22 mm, thickness ≈ 10 mm) were obtained by uniaxial pressing (10 MPa) and cold press (5 t during 3 min). For starch-loaded batches, a pre-burnout was carried out at 650 °C during 6 h and then all samples were dried at 120 °C for 4 h, sintered at 900 °C for 45 min, and finally furnace-cooled to room temperature. Dimensions were measured with a vernier caliper; mass and densities was obtained by a 50 mL pycnometer and Archimedes methods. Furnace temperature was confirmed with an independent K-type thermocouple and the universal testing machine (2 mm/min crosshead speed) was calibrated using standard blocks prior to testing.

RESULTS

Density, compressive strength, water absorption and thermal conductivity (S1–S6) of the six samples were studied. These properties demonstrate the correlations between the elements of material composition, symmetries and structures, as well as performances. These results demonstrate the coupling of thermal, mechanical and environmental influences. The synergy of these properties underscores the care needed to tune materials for applications in which each strength can be maximized, and each weakness mitigated.

Figure 1 shows a decrease of the density and an increase of the water absorption can be observed for all samples. Density only slightly varies from S1 (2.1 g/cm³) to S3 (2.14 g/cm³), before dramatically reducing until a minimum of

Table 1. The proportions of components in each sample

Symbol	Waste glass (g)	Fly ash (g)	SiC (g)	Starch
S1	53.27	6.43	0.3	0%
S2	50.79	8.91	0.3	0%
S3	48.38	11.32	0.3	0%
S4	50.79	8.91	0.3	2%
S5	50.79	8.91	0.3	4%
S6	50.79	8.91	0.3	6%

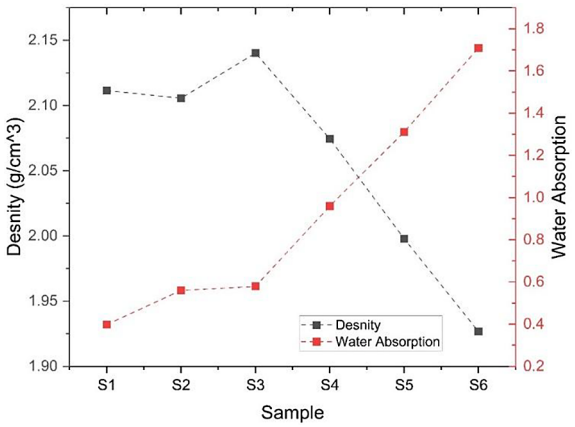

Figure 1. The variation in Density and water absorption with respect to Samples

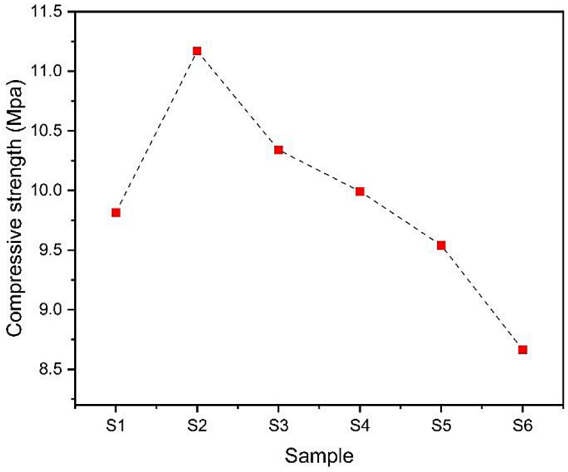

Figure 2. The variation in compressive strength with respect to Samples

1.92 g/cm^3 in case of S6. This reduction in density is coupled with a significant increase of water absorption, which increases from 0.39% for S1 to ~1.7% for S6. The significantly increased water absorption of the latter samples also reflects higher porosity. Materials with higher density (S1–S3) have lower porosity level, which enhances mechanical integrity. On the other hand, the lower densities and higher water absorption of S4–S6 imply a transformation towards lighter and more porous substance. This increase in porosity also corresponds to a greater starch content (27, 28) as the starch burns out on sintering (29), leaving behind porous structure. Such deformation improves characteristics, for example, insulation from heat.

The compressive strength of the samples, as depicted in Figure 2, takes the density-like behavior, expressing the structural accuracy of the materials. The maximum value of the compressive strength is attained for S2 (11 MPa) and then decreases with a tendency to a minimum average value of 8.5 MPa for S6. The decrease is more significant than after S3, which shows that structural changes in the material such as a greater porosity or when heavier elements are replaced by lighter components give poor mechanical properties. Such compressive strength trends are consistent with the density results, S1–S3 having naturally higher densities and therefore stronger resistance to compressive forces. For non-structural uses such as insulation panels or light partitions, S6 (with lower compressive strength) would be more adequate. It has been reported that increasing hydraulic porosity in the material results a lower compressive strength (30, 31).

'Mechanical' dimension Thermodynamic stability of such compositions is crucial for their long-term stability. A high compressive strength is desirable for maintaining the material's shape under pressure, such as in construction or industrial applications. The significant decrease in compressive strength between the second and first build layers S3 and S6 emphasizes the limitations due to the design decisions for this material, in particular when focusing on other properties such as thermal conductivity or weight reduction.

The samples' thermal conductivity (Figure 3), indicates a clear reduction from S1 to S6 and distinct differences between the low and high samples. Between S1 to S3, the thermal conductivity value for temperature 0.24–0.25 W/m·K which is nearly a constant representing no changes in structure or chemical content (17). But at S4~S6, a drastic decrease can be seen as thermal conductivity drops sharply to around 0.1 W/m·K for S6.

This dramatic reduction is very likely due to the later samples being engineered based on increased thermal insulation, such as a higher apparent porosity and finer closed-cell networ or more insulating materials with higher apparent porosity. This is particularly important in applications where decreasing heat transfer is desirable such as thermal barriers and insulation material. For instance, the lower thermal conductivity of S6 makes it particularly well-suited for these applications. Using starch as a pore-forming agent led to an increase in the number of pores in the S3, S4, and S6 samples. In porous materials, these pores can either contain a vacuum or be filled with gas (32).

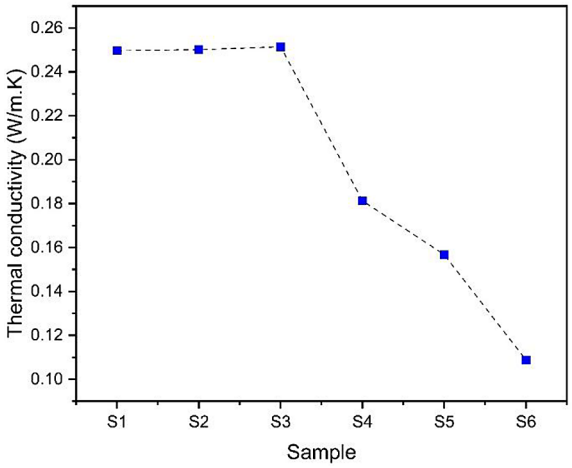

Figure 3. The variation in thermal conductivity with respect to Samples

In physics, phonons have responsibility for transferring heat energy through solids. Phonon movement can be hindered by defects including vacancies, impurities, dislocations, and alloy atoms (33–35), as well as grain boundaries (33) and pores (24), as shown in Figure 4. Phonons are categorized into two main types: optical and acoustic, with optical phonons dominating at higher temperatures and acoustic phonons at lower temperatures. Acoustic and optical components of phonon energy travel longitudinally and transversely in the bulk material. The pores and grain boundaries in the porous structure can cause phonon scattering, disrupting the phonons' mean free paths at the meso and micro scales (35). The decrease in thermal conductivity is primarily because of density lowering. The random distribution of holes and dense regions throughout the sample disrupts phonon propagation, reducing the phonons' mean free path (36), which in turn lowers lattice thermal conductivity (29, 37). Thus, the thermal conductivity and compressive strength observed are higher and more favorable compared to previous findings (17).

Increasing starch content systematically increased pore formation (via starch burnout), which reduced bulk density and enhanced phonon scattering, thereby lowering thermal conductivity from ~0.24–0.25 to 0.109 W/m·K at 6 wt% starch, while concurrently decreasing compressive strength from ~11.2 to ~8.7 MPa and increasing water absorption. This trade-off is consistent with foam-glass and porous-ceramic literature, where higher porosity decreases heat transport but compromises mechanical integrity (19, 24–26, 30, 31). The magnitude of thermal-conductivity reduction aligns with prior FAGF reports using waste glass/fly ash and foaming agents (17, 19, 20), while the achieved strength at 6 wt% starch remains within the range deemed acceptable for non-structural insulation panels. Moreover, the observed sensitivity of water uptake to porosity agrees with studies employing starch or similar pore formers (27–29). Collectively, these comparisons indicate that starch is an effective, natural, and tunable pore-forming additive for fly ash–waste glass systems, enabling insulation-oriented formulations without departing from the performance envelopes reported previously, yet with improved process simplicity (mix–press–sinter) and clear, statistically supported trends.

Most importantly, all these results suggest that starch-modified FAGF is a useful tunable insulating material (S6): continuously increasing concentration of starch (0–6 wt%) increases porosity and reduces thermal conductivity to 0.10875 W/m·K, while acceptably keeping its compressive strength (~8.66 MPa) appropriate for non-structural panels. The increase in insulating performance also resulted in an increased water uptake (from

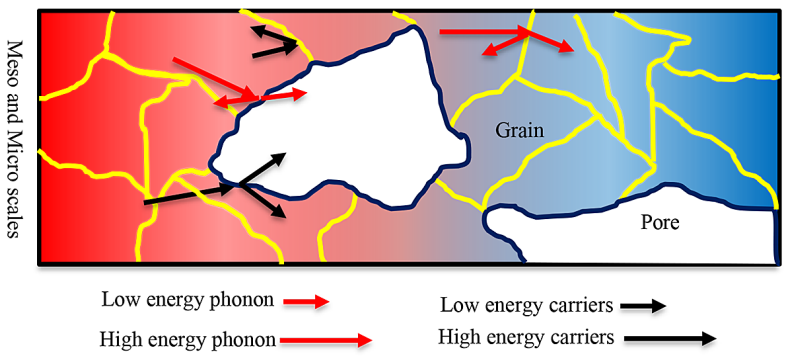

Figure 4. Schematic diagram of electronic transport and phonon scattering mechanisms from hot to cold side within a thermoelectric material at Meso and Micro scales

≈0.39% to ≈1.7%) and a moderate strength detriment; thus suggesting the importance of moisture protection or hydrophobic post-treatments in service. The present work is restricted to a small composition range (starch ≤6 wt%), one sintering schedule (900 °C, 45 min), and no detailed analysis of the microstructure (e.g., pore-size distribution) or long-term durability (e.g., freeze–thaw, thermal cycling). Future work needs to extend the processing window (starch amount/type, SiC content), combine SEM/porosimetry with property mapping and test mechanical and thermal stability under service relevant environments for broadening material application.

Statistical analysis of starch content effects

The descriptive statistics of Figures 1–3 were the first step towards an overview on how adding starch to the foam glass specimens influenced their physical and mechanical characteristics. These observations were confirmed by in depth statistical analysis with OriginPro software, which was performed on measured data using polynomial fit and ANOVA. Table shows the fitted model, residual analysis and regression coefficients. By using this strategy, any trends emerged in the raw data are not only visually if any but also statistically supported, therefore increasing robustness of the study.

However, by regression analysis it was confirmed that density is inversely related to starch content (2.14 g/cm³ in the absence of starch towards 1.93 at 6% s.). The fits of the polynomial model produced a very good determinant coefficient ($R^2 \approx 0.98$, Adj-$R^2 > 0.95$), which demonstrates that most variance between treatments could be attributed to starch addition. While the low number of replicates reduced the power of the statistical test, the residual plot and fitted curve supported uniformity in this down trend. This gives a quantitative confirmation of the pore forming contribution of starch, which could already be observed in the descriptive images.

The impact of starch on water uptake was unambiguous and statistically significant. The value of absorption varied between 0.39% in S1 to 1.71% in S6. The polynomial regression produced a good model fit ($R^2 = 0.9838$, Adj-$R^2 = 0.9731$) and showed a very high F-value ($F = 91.28$, $p = 0.0021$). The slope coefficient implies that for every 1% increase in starch, there is approximately a 0.22% increase in WA%. This confirms

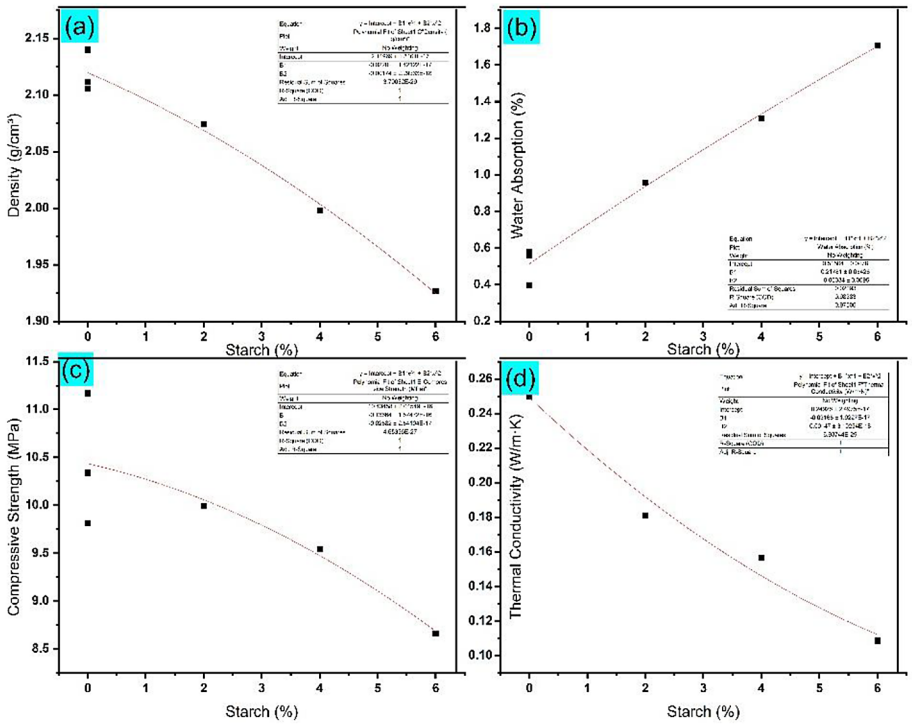

Figure 5. Polynomial regression fits showing the effect of starch content on (a) density, (b) water absorption, (c) compressive strength, and (d) thermal conductivity of fly ash–waste glass foam glass Black squares represent experimental data points, and red dashed curves denote the fitted regression models obtained from OriginPro. The regression parameters and statistical indicators are summarized in Table X.

the conclusion that porosity obtained from starch burnout plays a dominant role in water absorption, leading to an insulation benefit/moisture sensitivity trade off driven by porosity (Figure 5).

CONCLUSIONS

FAGF was synthesized by a simple process using waste glass and fly ash. The study reveals the fine correlation of thermal, mechanical and environmental behavior in the six samples. Samples S1-S3 have relatively higher density, compressive strength and thermal conductivity, which are applicable to structure with mechanical durability and low water absorption. On the other hand, comparing the 3 sets of samples S1 to S3 and S4 to S6, as the density and compressive strength decrease, thermal conductivity and water absorption increase. In these (S4–S6) porous samples, starch was added to enhance the porosity of the system, thereby decreasing their thermal conductivity and leading to better insulation. The best fraction was obtained for sample S6, for which 56% higher thermal conductivity was measured at the expense of reduction in compressive strength by 22%. With more starch addition, the integrity of the material became weaker and there was a greater risk for the samples to crush or deform. Nevertheless, the resulting product had good enough compressive strength and better thermal conductivity.

Acknowledgment

Acknowledgments. This work was partially supported by the College of Engineering, University of Basrah.

REFERENCES

1. Andrady AL. Plastics and the ocean: origin, characterization, fate, and impacts: Wiley Online Library; 2022.
2. Balaji G, Pavan PS, gautam D, Ashok P, Suganth V, Vetturayasudharsanan R. Utilization of lignite coal ash and steel slag in fly ash brick manufacturing: A review. IOP Conference Series: Earth and Environmental Science. 2022;1125(1):012015.
3. Yoon S-D, Lee J-U, Lee J-H, Yun Y-H, Yoon W-J. Characterization of wollastonite glass-ceramics made from waste glass and coal fly ash. Journal of Materials Science & Technology. 2013;29(2):149–53.
4. Zhang Z, Li Z, Yang Y, Shen B, Ma J, Liu L. Preparation and characterization of fully waste-based glass-ceramics from incineration fly ash, waste glass and coal fly ash. Ceramics International. 2022;48(15):21638–47.
5. Yousuf A, Manzoor SO, Youssouf M, Malik ZA, Khawaja KS. Fly ash: production and utilization in India-an overview. J Mater Environ Sci. 2020;11(6):911–21.
6. (EPA) USEPA. Guide to the Facts and Figures Report about Materials, Waste and Recycling 2018 [Available from: https://www.epa.gov/facts-and-figures-about-materials-waste-and-recycling/guide-facts-and-figures-report-about
7. Giergiczny Z. Fly ash and slag. Cement and Concrete Research. 2019;124:105826.
8. Zhang S, Shi T, Ni W, Li K, Gao W, Wang K, Zhang Y. The mechanism of hydrating and solidifying green mine fill materials using circulating fluidized bed fly ash-slag-based agent. Journal of Hazardous Materials. 2021;415:125625.
9. Taki K, Gahlot R, Kumar M. Utilization of fly ash amended sewage sludge as brick for sustainable building material with special emphasis on dimensional effect. Journal of Cleaner Production. 2020;275:123942.
10. Yuan Q, Robert D, Mohajerani A, Tran P, Pramanik BK. Utilisation of waste-to-energy fly ash in ceramic tiles. Construction and Building Materials. 2022;347:128475.
11. Yadav VK, Gacem A, Choudhary N, Rai A, Kumar P, Yadav KK, Abbas M, Khedher NB, Awwad NS, Barik D, Islam S. Status of coal-based thermal power plants, coal fly ash production, utilization in india and their emerging applications. Minerals. 2022;12(12):1503.
12. Rahma A, El Naber N, Issa Ismail S. Effect of glass powder on the compression strength and the workability of concrete. Cogent Engineering. 2017;4(1):1373415.
13. Al-Kheetan MJ, Byzyka J, Ghaffar SH. Sustainable valorisation of silane-treated waste glass powder in concrete pavement. Sustainability. 2021;13(9):4949.
14. Li C, Wang H, Fu C, Shi S, Liu Q, Xu P, Liu Q, Zhou D, Cheng Y, Jiang L. Effect and mechanism of waste glass powder silane modification on water stability of asphalt mixture. Construction and Building Materials. 2023;366:130086.
15. Ogunro A, Apeh F, Nwannenna O, Ibhadode O. Recycling of waste glass as aggregate for clay used in ceramic tile production. Am J Eng Res. 2018;7:272–8.
16. Hasan MR, Siddika A, Akanda MPA, Islam MR. Effects of waste glass addition on the physical and mechanical properties of brick. Innovative Infrastructure Solutions. 2021;6:1–13.

17. Song H, Chai C, Zhao Z, Wei L, Wu H, Cheng F. Experimental study on foam glass prepared by hydrothermal hot pressing-calcination technique using waste glass and fly ash. Ceramics International. 2021;47(20):28603–13.
18. Fan Y, Li S, Li Y, Liang H, Tang M, Huang K, Zhu L. Recycling of municipal solid waste incineration fly ash in foam ceramic materials for exterior building walls. Journal of Building Engineering. 2021;44:103427.
19. Cengizler H, Koç M, Şan O. Production of ceramic glass foam of low thermal conductivity by a simple method entirely from fly ash. Ceramics International. 2021;47(20):28460–70.
20. Li J, Zhuang X, Monfort E, Querol X, Llaudis AS, Font O, Moreno N, Ten FJG, Izquierdo M. Utilization of coal fly ash from a Chinese power plant for manufacturing highly insulating foam glass: Implications of physical, mechanical properties and environmental features. Construction and Building Materials. 2018;175:64–76.
21. Tang J, Wang H-T, Lee DH, Fardy M, Huo Z, Russell TP, Yang P. Holey silicon as an efficient thermoelectric material. Nano letters. 2010;10(10):4279–83.
22. Kashiwagi M, Hirata S, Harada K, Zheng Y, Miyazaki K, Yahiro M, Adachi C. Enhanced figure of merit of a porous thin film of bismuth antimony telluride. Applied physics letters. 2011;98(2).
23. Wang N, Han L, He H, Ba Y, Koumoto K. Effects of mesoporous silica addition on thermoelectric properties of Nb-doped SrTiO3. Journal of alloys and compounds. 2010;497(1–2):308–11.
24. Kim S, Lee H. Fabrication of conductive macroporous structures through nano-phase separation method. Electronic Materials Letters. 2018;14:83–8.
25. Raghavan S, Wang H, Dinwiddie RB, Porter WD, Mayo MJ. The effect of grain size, porosity and yttria content on the thermal conductivity of nanocrystalline zirconia. Scripta Materialia. 1998;39(8):1119–25.
26. Cha J, Kim D, Hong H, Kim G, Park K. Effect of La3+ substitution on the structural and thermoelectric properties of Ca3-xLaxCo4O9+ δ. Journal of the European Ceramic Society. 2019;39(11):3320–6.
27. Wu C, Li Z, Li Y, Wu J, Zhao Y, Liao Y. Effect of starch on pore structure and thermal conductivity of diatomite-based porous ceramics. Ceramics International. 2023;49(1):383–91.
28. Colak G, Leinders G, Vleugels J, Delville R, Verwerft M. Improved doping and densification of uranium oxide microspheres using starch as pore former. Journal of Nuclear Materials. 2023;577:154319.
29. Feng B, Li G, Pan Z, Xiaoming H, Peihai L, Zhu H, Yawei L. Effect of synthesis processes on the thermoelectric properties of BiCuSeO oxyselenides. Journal of Alloys and Compounds. 2018;754:131–8.
30. Anburuvel A, Subramaniam DN. Influence of aggregate gradation and compaction on compressive strength and porosity characteristics of pervious concrete. International Journal of Pavement Engineering. 2023;24(2):2055022.
31. Liao Z, Rabiee H, Ge L, Li X, Yang Z, Xue Q, Shen C, Wang H. Revelling pore microstructure impacts on the compressive strength of porous proppant based on finite and discrete element method. Journal of Materials Science & Technology. 2025;211:72–81.
32. Zhao K, Duan H, Raghavendra N, Qiu P, Zeng Y, Zhang W, Yang J, Shi X, Chen L. Solid-state explosive reaction for nanoporous bulk thermoelectric materials. Advanced Materials. 2017;29(42):1701148.
33. Sun H, Lv P, Wang C, Liu Y, Jia X, Ma H. HPHT synthesis and enhanced TE performance of Te and Sn/Se elements binary-doped $CoSb_3$. Functional Materials Letters. 2019;12(1):1850105.
34. Li Y, Li C, Wang B, Li W, Che P. A comparative study on the thermoelectric properties of CoSb3 prepared by hydrothermal and solvothermal route. Journal of Alloys and Compounds. 2019;772:770–4.
35. Zaferani SH, Ghomashchi R, Vashaee D. Strategies for engineering phonon transport in Heusler thermoelectric compounds. Renewable and Sustainable Energy Reviews. 2019;112:158–69.
36. Khan AU, Kobayashi K, Tang D-M, Yamauchi Y, Hasegawa K, Mitome M, Xue Y, Jiang B, Tsuchiya K, Golberg D. Nano-micro-porous skutterudites with 100% enhancement in ZT for high performance thermoelectricity. Nano Energy. 2017;31:152–9.
37. Zhou X, Yan Y, Lu X, Zhu H, Han X, Chen G, Ren Z. Routes for high-performance thermoelectric materials. Materials Today. 2018;21(9):974–88.